meropp@sandia.gov Avoiding asynchronous connections of adjacent microgrids in self-healing power systems

Michael Ropp
Sandia National Laboratories

Olga Lavrova
New Mexico State University

21, rue d'Artois, F-75008 PARIS
http : //www.cigre.org

CIGRE US National Committee
2023 Grid of the Future Symposium

Avoiding asynchronous connections of adjacent microgrids in self-healing power systems

M. Ropp[1], O. Lavrova[2], E. Silva[2]
[1]Sandia National Laboratories; [2]New Mexico State University
USA

SUMMARY

In self-healing, self-assembling power systems, in which adjacent microgrids may autonomously connect to one another (i.e., self-network), it is necessary to ensure that adjacent microgrids connect only when their voltages are sufficiently well-synchronized in magnitude and phase. In many cases, a standard synchronization check function can achieve this, but in self-healing power systems that rely on local measurements only (either due to lack of communications or due to a communications outage), situations arise in which two line relays form the boundary between two microgrids, and, because they cannot share data, neither can prevent the other from reclosing. It is thus necessary to ensure via the line relays' timing functions that they do not close at the same time, because if one closes first then the other can go to synchronization check. This paper describes a self-healing power systems concept utilizing only local measurements, describes and demonstrates how asynchronous connection of adjacent microgrids can occur, and then proposes a simple process for assigning "tagged" time delays to the line relays such that no two adjacent line relays have the same reclosure time delay. This "tagged timer" process is demonstrated via PSCAD simulation using the IEEE 13-bus distribution test circuit and manufacturer-specific, code-based inverter models.

KEYWORDS

Self-Healing Power Systems; Microgrids; Intentional Island Power Systems; Distributed Energy Resources; Protection; Microgrid Networking; IEEE 13-bus Distribution Test Circuit.

meropp@sandia.gov

INTRODUCTION AND BACKGROUND

A self-healing power system (SHePS) has the ability to automatically detect that it is not operating properly and restore as much of the system as possible to normal operation [1]. A SHePS must be able to perform a) protection, or detection and isolation of a fault; and b) restoration, in which all of the healthy parts of the system are re-energized. A great deal of work has been done on SHePS [2-6], and FLISR-type SHePS [7] are commercially available (for example, see [8] and [9]).

However, there is one significant drawback that is shared by nearly all of today's SHePS concepts: They generally rely on data sharing via high-speed networked communications [10]. Communications improve performance under "blue-sky" conditions, but a) they are expensive, often to the point of rendering projects unfeasible; and b) they can become unreliable during "black-sky" events. Maurer et.al. wrote in 2012: "Communications is the Achilles' Heal *(sic)* of any self-healing system. No matter what type of self-healing system you select—centralized, substation-based, or distributed intelligence—that fact is still true." [11] Concepts based on data sharing also often struggle with scalability and cybersecurity challenges. There is thus a need for SHePS technologies that rely on *local measurements only*, and that support ad-hoc networking of microgrids. However, when one is limited to local measurements only, two additional challenges appear. The first is that with SHePS energized entirely by distributed inverter-based resources (IBRs) including solid-state transformers, time-overcurrent protection, which is the most-used protection tool in distribution systems [13], becomes ineffective due to the fault current limitations of the power electronics [14]. Directional elements would generally be the next tool used, followed by distance relays [13], but these too become unreliable with geographically-distributed IBRs. When a fault occurs in a SHePS energized only by IBRs, what tends to happen is a systemwide undervoltage occurs because the IBRs reach their current limits and cease voltage regulation. This undervoltage tends to have a low gradient, rendering coordination difficult. Thus, in a system of this type, it is not difficult to detect the *existence* of a fault, but it is difficult to ascertain the fault's *location*.

The second challenge arises because today's restoration procedures are also designed around a centralized system architecture energized by rotating machines [15]. System restoration is a complex process that involves coordinating black-start resources, identifying critical paths, estimating surge loads during re-energization, and understanding the dynamics of the system at each step of the restoration process [16]. It is widely recognized that distributed resources can assist with system restoration, but most proposed techniques for achieving this still rely on centralized communication and control [16,17].

Investigators at Sandia National Laboratories and New Mexico State University have been collaborating on a project called "SHAZAM", in which a set of tools that facilitates creating self-assembling SHePS energized by distributed power electronics-based sources, using local measurements only [18,19,20], has been developed. The SHAZAM concept utilizes line relays, which sectionalize the system's main conductors, and load relays, which may be implemented in "smart meters" and which contain a number of automatic load-shedding functions. For example, Figure 1 shows a one-line diagram of the IEEE 13-bus distribution test circuit [21] configured to operate as a microgrid using this concept. The red blocks are closed relays. Each load has a load relay, and there are ten line relays, R1 through R10. This system has a microgrid isolation device, which is shown as green indicating that it is open and this system is off-grid.

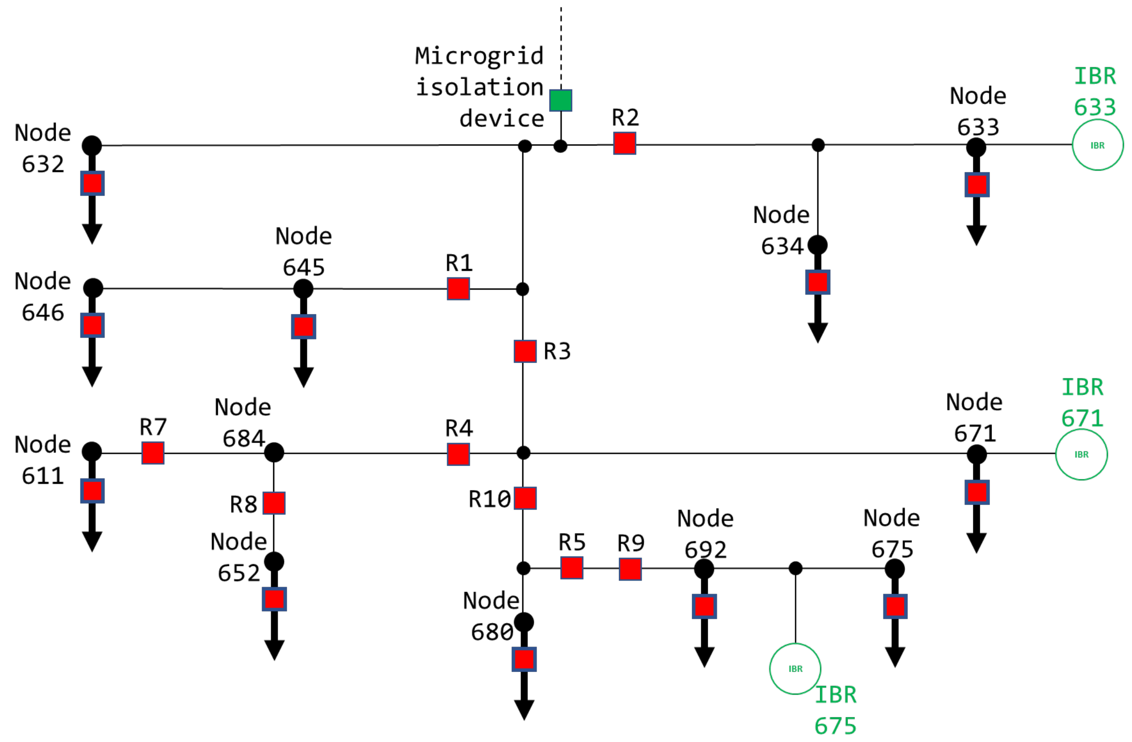

Figure 1. IEEE 13-bus distribution test circuit configured to operate as three microgrids, with an IBR (green) in each microgrid.

Consider a case in which a fault occurs near node 645, as shown in Figure 2. As discussed above, the IBRs hit their current limits and the entire system enters into an undervoltage condition. The first step toward restoring the system is undervoltage load shedding (UVLS, essentially an IEEE 27TD function [22]). The undervoltage functions in the load relays begin shedding load, with lower-priority loads having shorter trip times and being shed first. In Figure 2 (left), the first group of loads (least critical) has been shed, as indicated by the green-filled load relays. The fault persists, so the undervoltage remains, and some time later the second group of loads is shed on UVLS, as shown in Figure 2 (right). The fault persists, and the undervoltage condition remains. At this point, after UVLS has been exhausted, the line relays' time-undervoltage (27TD) functions then disassemble the SHePS into local intentional islands, each centered around a grid-forming IBR, as shown in Figure 3. The green dashed lines in Figure 3 show the boundaries of the three microgrids. There is a line relay on the boundary of each microgrid—for example, the boundary of Microgrid 633 includes line relay R2, and the boundary of Microgrid 671 includes line relay R3. When a line relay sees an in-range voltage on one side that remains stable for a preset length of time, then that line relay can reclose. In Figure 4 (left), line relays R2, R3, R4, R9 and R10 each sees an in-range voltage on one side, and they can all reclose, resulting in the new microgrid boundaries shown in Figure 4 (left). At this point, R1, R7 and R8 each see in-range voltage on one side only and can reclose on a timer, as shown in Figure 4 (right). Now, line relay R5 sees in-range voltage on both sides and will only reclose when two conditions are met: a) a synchronization check function (IEEE function number 25 [22]) has verified that the voltages on each side of the relay are sufficiently similar in magnitude and the phase angle difference between them is sufficiently small; and b) an unintentional loop detection function has verified that closure of that relay will not create a closed loop in a system designed to be operated radially [18]. In Figure 4 (right), note that line relay R1 has reclosed onto the fault. When this happens, the system voltage collapses again, and line relay R1 sees significant fault current immediately upon its closure. At this time, a windowed undervoltage-supervised overcurrent function (UVOC, IEEE function number 51V [22]) asserts itself: if a line relay, having reclosed due to in-range voltage on one side only, sees a voltage collapse accompanied by high current within a short time window (here, 300 ms) after its closure, that line relay re-opens and locks out. In this way, the fault is isolated (Figure 5, left). The UVOC or 51V function timing must be long enough that it is not activated by the various inrush currents associated with cold load pickup. Eventually the synchronization check function (function 25) in line relay R5 is satisfied, and it recloses. No generation has been lost, so there is sufficient capacity to recover all of the loads, and the final system state is as shown in Figure 5 (right). With the SHAZAM SHePS concept, all loads for which there is sufficient generation and intact source-load paths can be back online [18,19] within minutes after a major disruption.

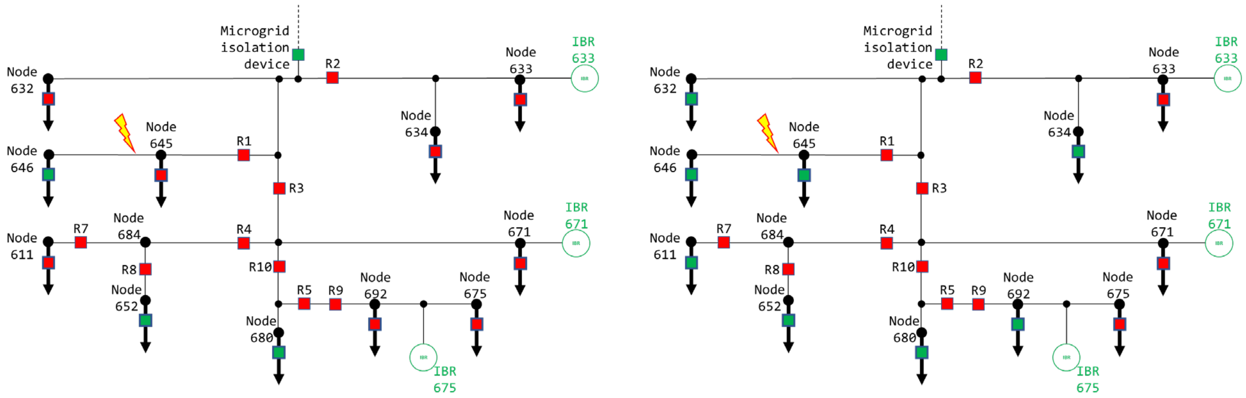

Figure 2. The system in Figure 1, undergoing a fault. Left : system after the first phase of UVLS (shedding Priority C loads). Right : system after the second phase of UVLS (shedding Priority B loads).

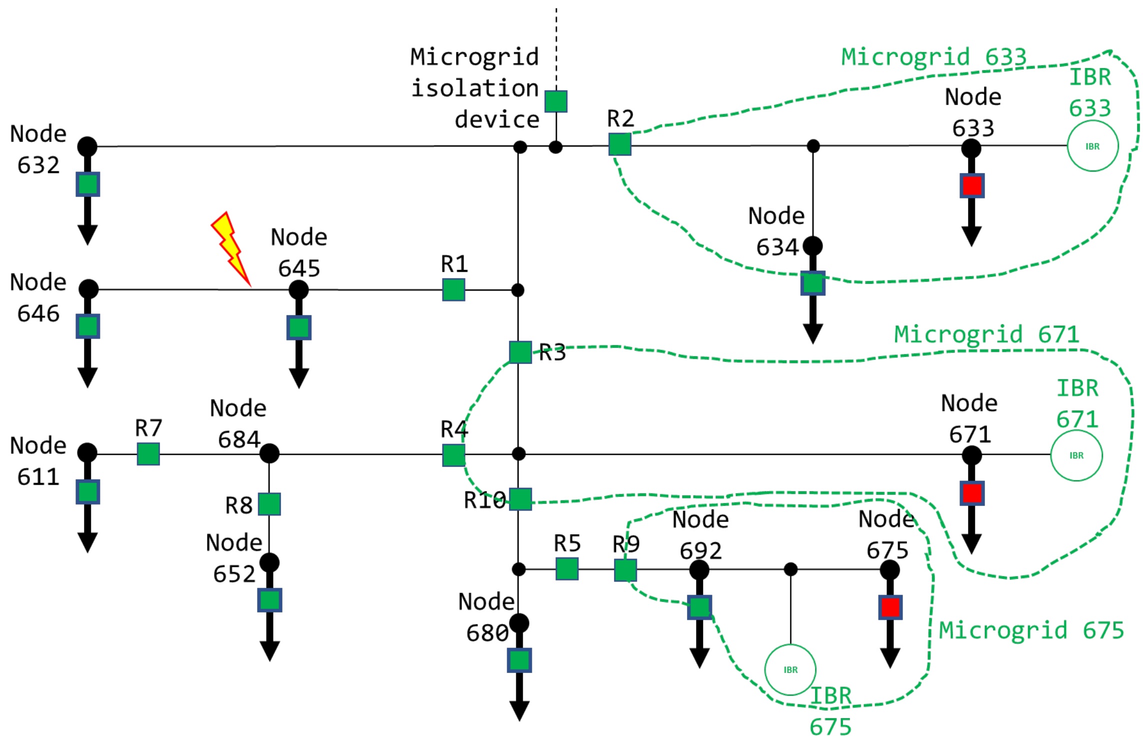

Figure 3. After UVLS has been exhausted, the line relays all open on undervoltage, creating three isolated microgrids each centered around a grid-forming IBR. The microgrid boundaries are shown in dashed green.

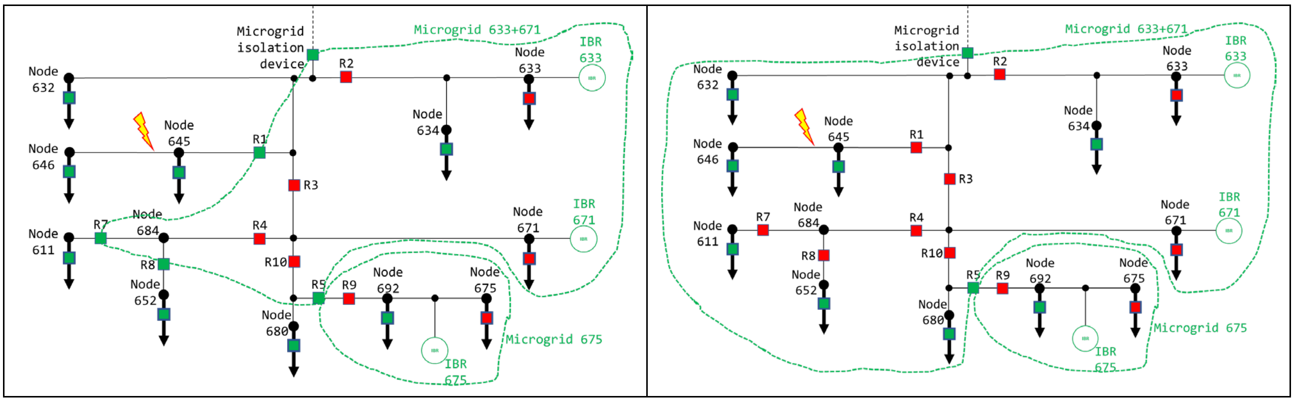

Figure 4. Line relays that see in-range voltage on one side only are allowed to reclose, expanding the microgrid boundaries. Left : R2, R3, R4, R9, and R10 close. Right : R1, R7 and R8 close (note that R1 closes onto the fault).

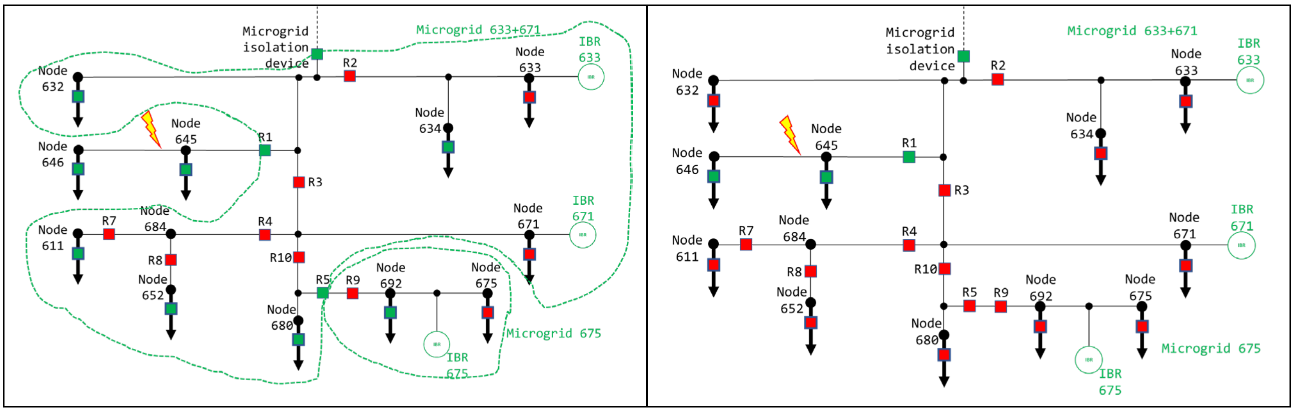

Figure 5. Left : Line relay R1 re-opens on UVOC, and locks out to isolate the fault. Right : Final system state after self-assembly has been completed.

PROBLEM STATEMENT

During self-assembly of multi-source microgrids, one condition that must be avoided is an asynchronous connection of two adjacent microgrids. In Figure 5 (left), line relay R5 is on the boundary between microgrid 675 and the combined microgrid 633+671, and it sees in-range voltage on both sides. If there is a significant difference in the magnitudes or phase angles of the voltages on either side of R5 when it closes, then large currents could surge back and forth between the microgrids, potentially leading to transient instability in the microgrids and likely triggering the UVOC function in relay R5. To avoid such an asynchronous connection, the line relays all incorporate a standard synchronization check or "sync-check" function (IEEE function number 25) in which the relay will not close until the magnitudes and phase angles of the voltages on either side of the relay are within preset tolerances. For IBR-energized systems, the required values of these tolerances will be set by the need to avoid damage to rotating loads in the microgrids.

However, in Figure 3, the boundary between microgrids 633 and 671 passes between line relays R2 and R3. Thus, in this situation, R2 and R3 together form the border between microgrids 633 and 671, and they must not be allowed to close simultaneously because this could create an asynchronous connection between microgrids 633 and 671. Because the line relays are using local measurements only, it is not possible to block one relay or the other via shared data. Thus, the timers used to close the line relays when they see in-range voltage on one side only must be configured such that no two adjacent line relays have exactly the same timing interval. In this way, one of the two line relays will always close first, and the other will then see in-range voltage on both sides and go to its synch-check function, preventing the asynchronous connection.

One method for differentiating the line relay closure timers would be to add a random element to the timers. However, there is still a finite possibility that two adjacent line relays could choose the same random delay, and if the resolution of the random timers is relatively coarse, which it would have to be to ensure that there is a sufficient time delay between any two adjacent line relays, then the probability that two adjacent line relays can choose the same random delay becomes significant [18]. As will be demonstrated below, the random time element is often not sufficient to guarantee prevention of asynchronous closure.

PROPOSED SOLUTION

The solution proposed is to add to the line relay closure time a 'tagged time', which is calculated as follows:

$$t_{reclose} = t_{fixed} + t_{tagged}$$
$$t_{tagged} = t_{inc} \times k$$

where $t_{reclose}$ is the reclose delay applied for in-range voltage on one side only, t_{fixed} is a fixed delay (typically 2-5 seconds), t_{tagged} is the tagged time, t_{inc} is a pre-selected timing increment that is much shorter than t_{fixed} (in this paper, t_{tagged} = 300 ms), and k is the tag, which is an integer between 0 and 2 that multiplies t_{inc}. Each line relay is assigned a value of the tag k, according to the following procedure:

1. Set the tag number to 0.
2. Start from each grid-forming IBR.
3. Move outward along the circuit conductors, including any branches, until a line relay is reached on each branch. If there are no branches, then this set will contain only one line relay.
4. For each set of line relays found in step 3, check to see whether any two of them are adjacent (i.e., any two line relays with no other line relay between them).
   a. For each line relay that is not adjacent to any line relay associated with another IBR, assign it the tag number k.
   b. If there are any two line relays that are adjacent as described above, assign k to one, and $k + 1$ to the other.
5. Increment the tag number by 1. If the tag number = 3, reset the tag number to zero.
6. Have all line relays been assigned a tag number? If so, stop. If not, return to Step 3.

This procedure is shown in flowchart form in Figure 6. The procedure ensures that, in the presence of multiple sources, no two adjacent relays have the same value of tagged time, and thus no two adjacent relays will ever close at the same time, preventing asynchronous connections.

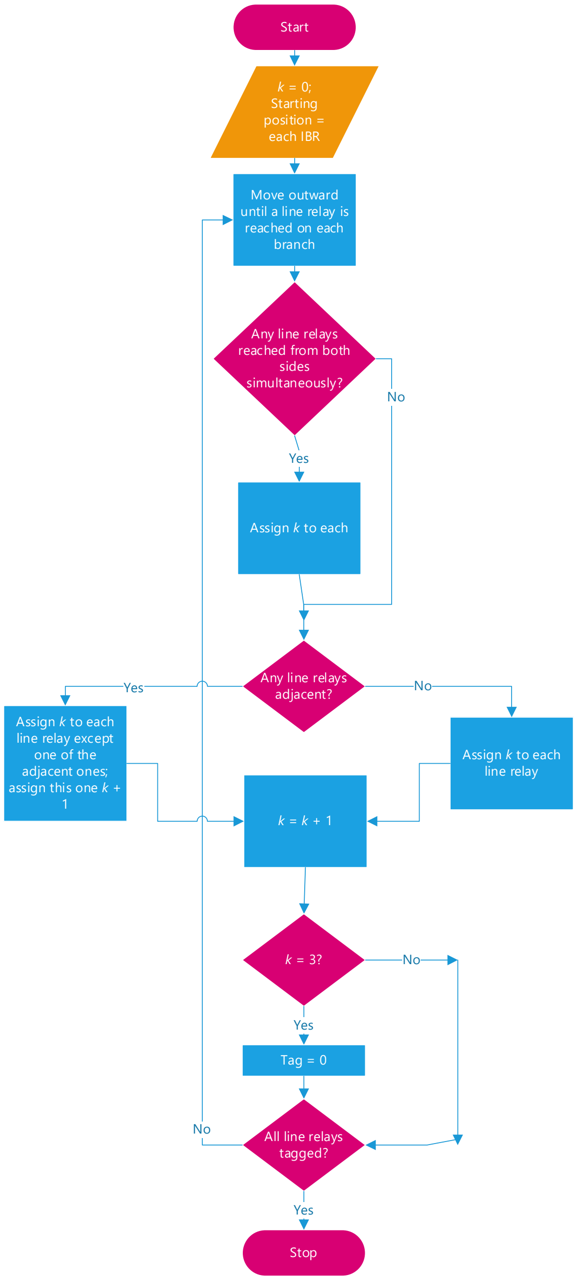

Figure 6. Flowchart of the process for assigning timer tags to the line relays.

Figure 7 and Figure 8 demonstrate the application of this process to the IEEE 13-bus distribution test circuit system shown in Figure 1. The process starts with $k = 0$, then moves outward from each IBR along each branch until we reach a line relay, as shown by the boundaries drawn in Figure 7. For IBR 633, line relay R2 is reached in this first iteration of step 3, and for IBR 675 line relay R9 is reached in this step. For IBR 671, line relays R3, R4 and R10 are reached simultaneously. Next, one checks whether any two line relays are adjacent (Step 4). In this case there is one adjacent pair : R2 and R3. One of these must be assigned $k + 1$, so in this example R2 is chosen to be tagged with $k + 1$, and the others (R3, R4, R9 and R10) are each assigned $k = 0$. The value of k is incremented to $k = 1$ (step 5), which is still less than 3.

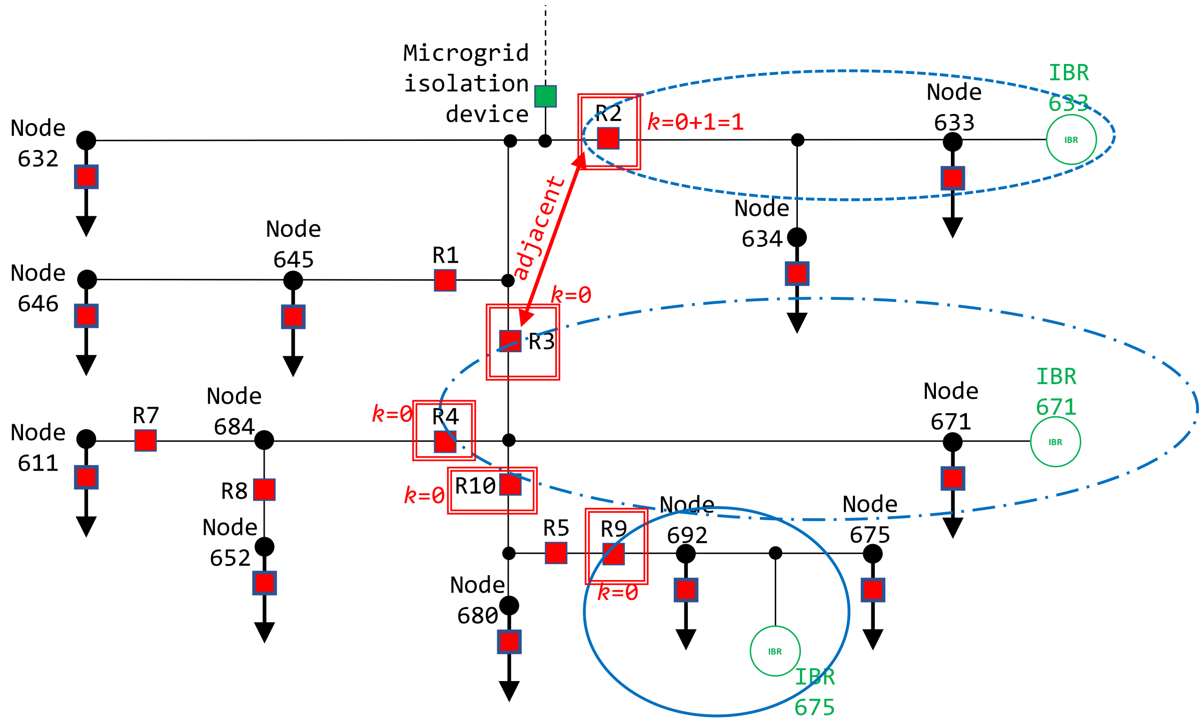

Figure 7. First step in assigning tag values to the line relays. R2 and R3 are adjacent, so one of the two (R2 is selected here) receives a tag value of $k + 1$.

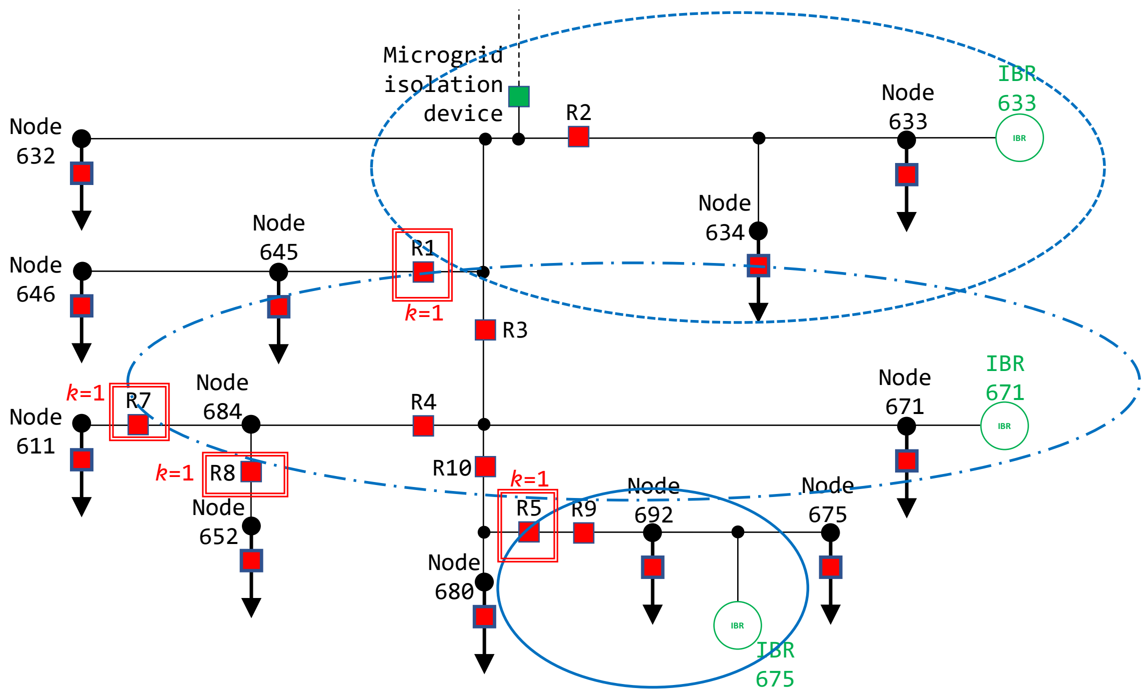

Figure 8. Second step in assigning tag values to the line relays. At this point, all relays have tag values, so this is the final step for this system.

Not all of the line relays have been assigned tag values (step 6), so the process repeats back to step 3, in which the boundaries are moved away from each IBR by one line relay, resulting in the boundaries shown in Figure 8. R1, R5, R7 and R8 each receive tag values of $k = 1$. No line relays are adjacent in this case (Step 4). The tag value is incremented to $k = 2$. At this point, all of the line relays have assigned tag values, so the process is complete.

DEMONSTRATION

Asynchronous connection using random timers

Figure 9 and Figure 10 show results from a PSCAD simulation in which the line relays in the IEEE 13-bus distribution test circuit (Figure 1) have fixed and random timing elements, but

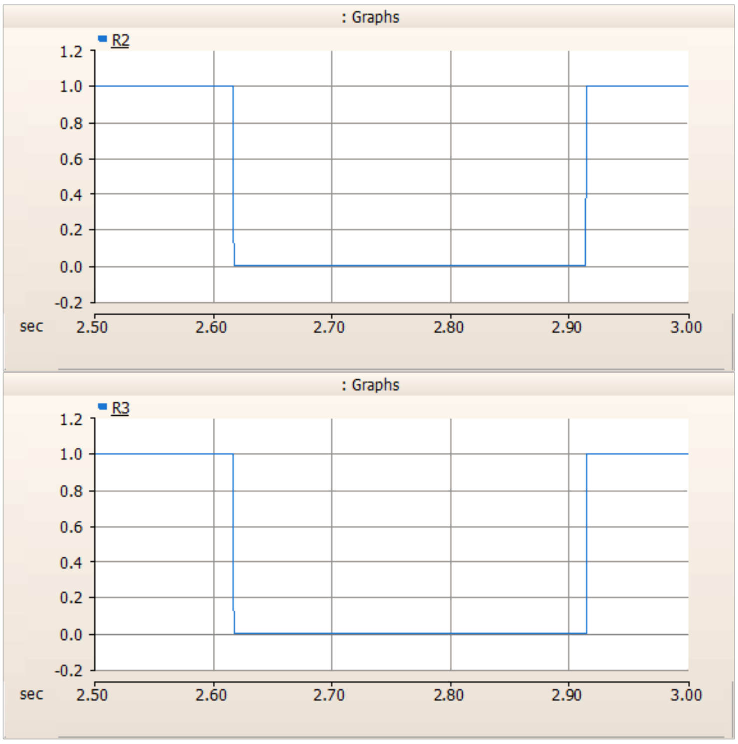

Figure 9. Breaker control signals for R2 and R3 during a black start, using the random timer element and not the tagged timer element. (In PSCAD, a 0 indicates a closed breaker, and 1 is open.)

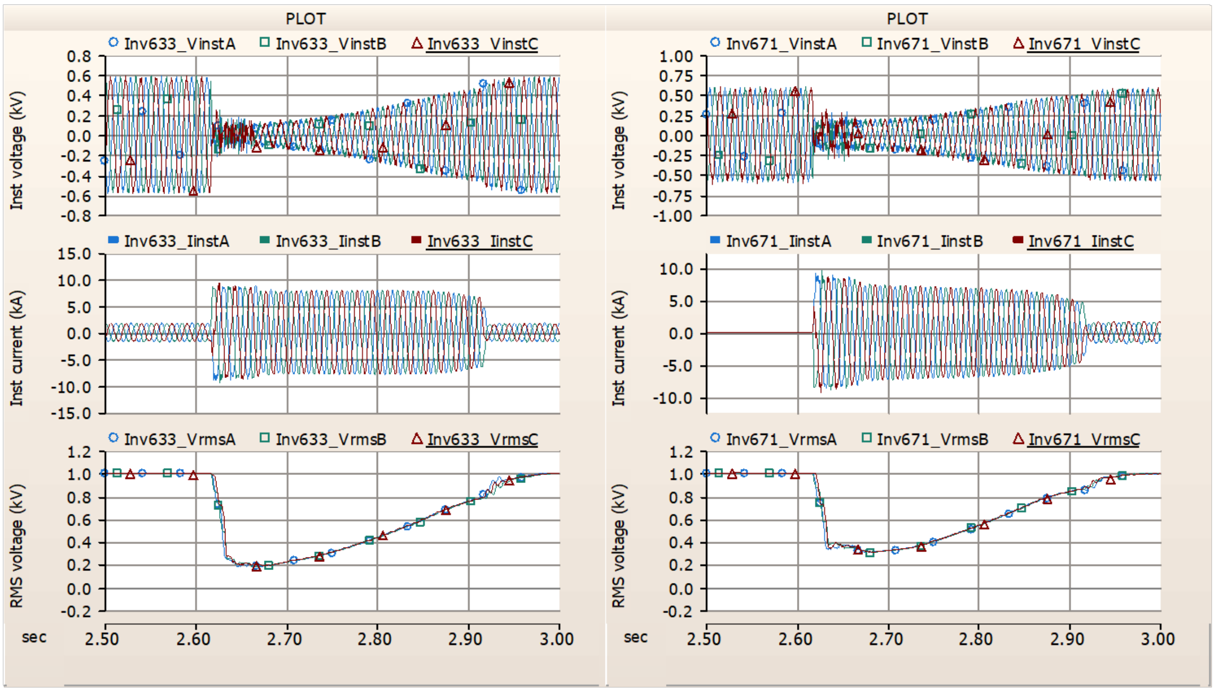

Figure 10. Instantaneous voltage (top), instantaneous current (middle), and RMS voltage (bottom) at IBRs 633 (left) and 671 (right) during an asynchronous connection of microgrids 633 and 671.

not the tagged timers. The three IBRs (Figure 1) are represented using detailed, code-based, manufacturer-supplied black-box inverter models. After a large number of simulations was run, one case was observed in which line relays R2 and R3 selected the same random time delay. During black start, both relays attempted to close at the same time (Figure 9), resulting in an asynchronous connection of microgrids 633 and 671. Figure 10 shows the instantaneous voltage, instantaneous current, and RMS voltage measured on the low-voltage buses of IBRs 633 (left) and 671 (right). The asynchronous connection leads to a voltage collapse and a large surge in current. This simultaneous voltage collapse and surge current triggers the UVOC functions in R2 and R3, both of which re-open (Figure 9) and lock out. This demonstrates the need to avoid such asynchronous connections.

Avoidance of asynchronous connection using tagged timers

Figure 11 shows results from a PSCAD simulation using the IEEE 13-bus distribution test circuit (Figure 1), using the fixed and tagged time delay elements. The left plot in Figure 11 shows the line relay closure timings during black start of the system. R2 and R3 are adjacent, and their closure times are in the red dashed circle. They are widely separated because R3 closed first ($k = 0$), after which R2 ($k = 1$) detected in-range voltage on both sides and closed on sync check roughly 11.5 seconds later. Similarly, R5 and R10 are adjacent, and their closure timings are circled in dashed green. The same situation occurs here: R10 ($k = 0$) closes first, and R5 ($k = 1$) then sees in-range voltage on both sides and closes on sync check just under 8 seconds later. The right plot in Figure 11 shows the line relay reclosure timings during system self-reassembly following a single line to ground (SLG) fault at node 633. This fault causes IBR 633 to become disconnected from the rest of the system. Line relay R3 ($k = 0$) closes first, at just after $t = 24.5$ s. Just over 2 seconds later, R2 ($k = 1$) closes on sync check, but it recloses onto the fault. The UVOC (51V) function asserts itself and R2 re-opens less than 200 ms later, isolating the fault. (R3 does not open because the undervoltage-overcurrent combination occurs outside of its UVOC window.)

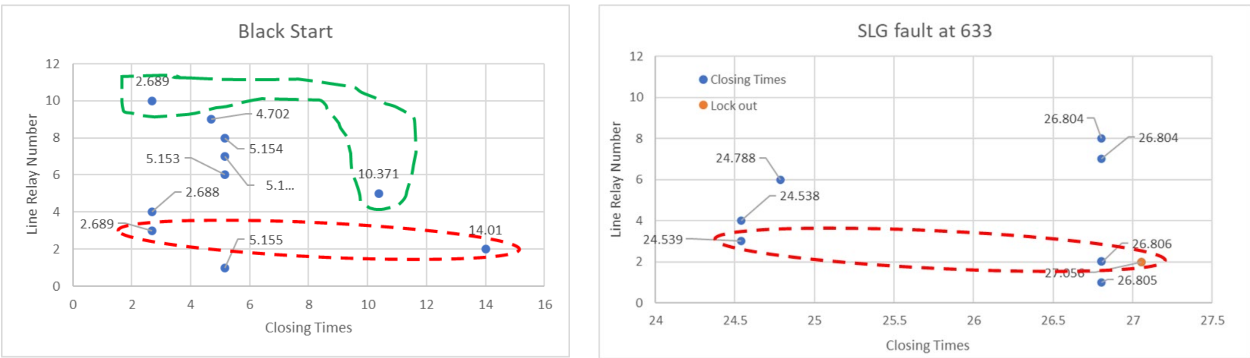

Figure 11. Closing times of the line relays in the IEEE 13-bus distribution test circuit (Figure 1), during black start (left) and reassembly after an SLG fault at node 633 (right).

CONCLUSION

In self-healing power systems that a) utilize only local measurements and b) in which microgrids can automatically connect to one other (i.e., self-network), situations can arise in which two line relays together form the boundary between two adjacent microgrids, and it is necessary to prevent these relays from closing at the same time in order to avoid an asynchronous connection of the two microgrids. This paper describes a self-healing systems concept using only local measurements, demonstrates the above-described problem, and proposes a simple solution using a procedure to assign « tagged timers » to the line relays, ensuring that no two adjacent relays have the same reclose delay. The use of « tagged timers » was demonstrated in PSCAD using the IEEE 13-bus test circuit and manufacturer-specific code-based IBR models. The tagged timers successfully avoided an asynchronous reclosure in a situation in which using a random timer element was not sufficient.

ACKNOWLEDGMENT
The authors gratefully acknowledge the key contributions of Raymond Byrne (Sandia National Laboratories) to the tagged timer concept.

This work was supported by the Laboratory Directed Research and Development program at Sandia National Laboratories, a multimission laboratory managed and operated by National Technology and Engineering Solutions of Sandia LLC, a wholly owned subsidiary of Honeywell International Inc. for the U.S. Department of Energy's National Nuclear Security Administration under contract DE-NA0003525.

BIBLIOGRAPHY

[1] D. Ghosh, R. Sharman, H. Rao, S. Upadhyaya, "Self-Healing Systems—Survey and Synthesis", *Elsevier Decision Support Systems* **42** 2007, p. 2164-2185.

[2] Li, Z. Chen, L. Fan, P. Zhang, "Toward A Self-Healing Protection and Control System", 40th North American Power Symposium, Sept 2008.

[3] Y. Liu, R. Fan, V. Terzija, "Power System Restoration: A Literature Review From 2006 to 2016", *Journal of Modern Power Systems and Clean Energy* **4**(3), July 2016, p. 332-341.

[4] R. Campos, C. Figueroa, H. Oyarzun, J. Baeza, "Self-Healing of Electric Distribution Networks: A Review", 7th IEEE International Confernece on Computers Communications and Control (ICCCC), May 2018.

[5] M. Elgenedy, A. Massoud; S. Ahmed, "Smart grid self-healing: Functions, applications, and developments", *First IEEE Workshop on Smart Grid and Renewable Energy (SGRE),* March 2015.

[6] S. Refaat, A. Mohamed, P. Kakosimos, "Self-Healing Control Strategy: Challenges and Opportunities for Distribution Systems in Smart Grid", 12th IEEE International Conference on Compatibility, Power electronics and Power Engineering, April 2018.

[7] J. Liu, X. Dong, X. Chen, X. Tong, X. Zhang, S. Xu, Fault Location and Service Restoration for Electrical Distribution Systems, pub. Wiley 2016, 978-1-118-95025-8.

[8] S&C Electric Intelliteam, https://www.sandc.com/en/products--services/products/intelliteam-sg-automatic-restoration-system/.

[9] SEL's "DNA", https://cms-cdn.selinc.com/assets/Literature/Publications/Case%20Studies/LCS0030_Westar%20Energy%20Case%20Study_20141103.pdf?v=20161024-215235.

[10] D. Lagos, V. Papaspiliotopoulos, G. Korres, N. Natziargyriou, "Microgrid Proection Against Internal Faults", *IEEE Power and Energy Magazine* May/June 2021, p. 20-35.

[11] L. Maurer, A. Stevens, W. Reder, "Tales From the Frontline: Keys to Successful Self-Healing Distribution Projects", *IEEE Power and Energy Magazine* **10**(2), March/April 2012, p. 100-106.

[12] L Yang, F. Xiao, H. Chen, Y. Lai, Y. Chollot, "The Experiences of Decentralized Self-Healing Grid", 8th IEEE International Conference on Advanced Power System Automation and Protection (APAP), October 2019.

[13] P. Anderson, Power System Protection, New York, NY: IEEE Press, 1999, ISBN 978-0-78-033427-4.

[14] M. Reno, S. Brahma, A. Bidram, M. Ropp, "Influence of Inverter-Based Resources on Microgrid Protection (Part 1)", *IEEE Power and Energy Magazine* **19**(3), May/June 2021, p. 36-46.

[15] Y. Liu, R. Fan, V. Terzija, "Power System Restoration: a Literature Review from 2006 to 2016", *Journal of Modern Power Systems and Clean Energy* **4**(3), July 2016, p. 332-341.

[16] K. Sun, Y. Hou, W. Sun, J. Qi, Power System Control Under Cascading Failures, pub. IEEE Press 2019, ISBN 978-1-119-28202-0.

[17] J. Brombach, C. Hachmann, D. Lafferte, A. Klingman, W. Heckmann, F. Welck, D. Lohmeier, H. Becker, "The Future of Power System Restoration", *IEEE Power and Energy Magazine* Nov/Dec 2018, p. 30-41.

[18] M. Ropp, M. Reno, M. Biswal, "Detection and Prevention of Unintentional Formation of Loops in Self-Healing Power Systems and Microgrids", *IEEE Transactions on Power Delivery* (early access), March 15 2023.

[19] E. Silva, O. Lavrova, M. Ropp, "Protection Elements for Self-Healing Microgrids Using Only Local Measurements", Proceedings of the 2022 North American Power Symposium (NAPS), Oct 2022.

[20] M. Ropp, O. Lavrova, S. Ranade, A. Ramoko, C. Valdez, "Results of Late-Start LDRD Project 'SHAZAM'", Sandia National Laboratories report SAND2021-11593, available online at https://www.osti.gov/servlets/purl/1821319

[21] IEEE PES Test Feeder web site, https://cmte.ieee.org/pes-testfeeders/resources/.

[22] IEEE Std C37.2-2008, "IEEE Standard for Electrical Power System Device Function Numbers, Acronyms, and Contact Designations".